International Journal of Minerals, Metallurgy and Materials
Volume 26, Number 4, April 2019, Page 430
https://doi.org/10.1007/s12613-019-1733-9

Process mineralogy as a key factor affecting the flotation kinetics of copper sulfide minerals

Ataallah Bahrami[1)], *Mirsaleh Mirmohammadi*[2)], *Yousef Ghorbani*[3)], *Fatemeh Kazemi*[1)], *Morteza Abdollahi*[1)], *and Abolfazl Danesh*[4)]

1) Department of Mining Engineering, Urmia University, Urmia P.O. Box 57561/51818, Iran
2) School of Mining Engineering, College of Engineering, University of Tehran, Tehran P.O. Box: 1439957131, Iran
3) Department of Civil, Environmental & Natural Resources Engineering, Luleå University of Technology, Luleå SE-971 87, Sweden
4) Complex of Copper Processing-Sungun, East Azerbaijan Province, Headquarters Rd, Tabriz-Iran
(Received: 10 May 2018; revised: 6 September 2018; accepted: 7 September 2018)

Abstract: The aim of this study is to apply process mineralogy as a practical tool for further understanding and predicting the flotation kinetics of the copper sulfide minerals. The minerals' composition and association, grain distribution, and liberation within the ore samples were analyzed in the feed, concentrate, and the tailings of the flotation processes with two pulp densities of 25wt% and 30wt%. The major copper-bearing minerals identified by microscopic analysis of the concentrate samples included chalcopyrite (56.2wt%), chalcocite (29.1wt%), covellite (6.4wt%), and bornite (4.7wt%). Pyrite was the main sulfide gangue mineral (3.6wt%) in the concentrates. A 95% degree of liberation with d_{80} > 80 μm was obtained for chalcopyrite as the main copper mineral in the ore sample. The recovery rate and the grade in the concentrates were enhanced with increasing chalcopyrite particle size. Chalcopyrite particles with a d_{80} of approximately 100 μm were recovered at the early stages of the flotation process. The kinetic studies showed that the kinetic second-order rectangular distribution model perfectly fit the flotation test data. Characterization of the kinetic parameters indicated that the optimum granulation distribution range for achieving a maximum flotation rate for chalcopyrite particles was between the sizes 50 and 55 μm.

Keywords: microscopic analysis; flotation; kinetics; second order rectangular distribution model; sulphide minerals

1. Introduction

Mineralogical studies on mineral deposits of an ore lead to a proper interpretation of metallurgical problems in the design of the processing circuit [1]. Process mineralogy is an integrated discipline that combines quantitative (and qualitative) mineralogical techniques with metallurgical test work [2–3]. Modern process mineralogy has been making substantial advances in methodology and data interpretation since it was first developed in the mid-1980s as a multi-disciplinary team approach to obtaining mineralogical information from drill-core and plant samples to infer the metallurgical processing requirements of an ore. The aim of the process mineralogist is to provide information about specific aspects of the ore mineralogy and mill products and, in so doing, to assist the chief metallurgist in optimizing metallurgical flowsheets [4–5].

Several studies have emphasized the importance of process mineralogy in mineral processing [6–19]. In recent years, mineral detection technology has been used to reduce the risk of designing new circuits and to detect and correct the low efficiency of flotation and leaching circuits; in practice, it is used to optimize processing operations in mines with different deposits [5,9–10]. Therefore, applying process mineralogy could provide inclusive information about the texture and structure of minerals and their behavior during the flotation process, such as their ability to respond effectively to the flotation process, their retrieval, and, consequently, the trend of flotation kinetics of ore particles.

Froth flotation is a physicochemical process that has been

Corresponding author: Yousef Ghorbani E-mail: Yousef.Ghorbani@ltu.se

used for more than a century in the concentration of copper sulfide minerals [20]. This technique is based on the wettability of minerals and is designed to recover the mineral species of interest and depress unwanted gangue [21]. One of the important aspects of the flotation process is its kinetics. The quantification of kinetic parameters is becoming increasingly important for shedding light on the speed of industrial flotation processes [22–23]. Flotation operations, as well as the associated kinetic and thermodynamic phenomena, are random processes. In general, the number of particles that permanently attach to a bubble's surface causes the kinetic parameter to depend on time [23–25]. Additionally, an individual mineral may have different characteristics under different geological conditions and exhibit different behaviors in flotation processes, which has received less attention in previous studies.

The aim of the present study is to use process mineralogy as a practical tool for further understanding and predicting the flotation kinetics of copper sulfide minerals. For this purpose, comprehensive mineral characterization studies were conducted using microscopic analysis of selected samples of feed, concentrates, and tails. The most important sample characteristics were determined to be the particle size distribution, the grains distribution and liberation, and associated minerals as the key rate-limiting factors in the kinetic behavior of the flotation process from a process mineralogy viewpoint.

Finally, the flotation behavior of copper ore is interpreted on the basis of the obtained results to provide recommendations for improving the effectiveness of the flotation process unit in practical operation.

2. Experimental

2.1. Ore samples

Ore samples were collected from the Sungun porphyry copper deposit, northwest of Iran, at latitude 38°43′ N and longitude 46°43′ E. This deposit contains more than 750 million tons of sulfide ore with 0.76wt% of copper and 0.01wt% of molybdenum (approximately). The intrusion of Sungun stoke in the upper Cretaceous has caused severe cracks in both the deposit and the surrounding rocks; it has also resulted in subsequent phases of alteration and mineralization, forming a porphyry–skarn-type ore deposit in Sungun. Three kinds of mineralization zones can be detected in Sungun: leached, supergene, and hypogene. Extremely large fractures and abundant sulfide minerals in these rocks have substantially affected the alteration factors. As a result of this process, the supergene zone is divided into oxidized leached zones in the top section and a sulfide-rich lower part minerals zone [26]. Minerals such as goethite, hematite, limonite, jarosite, malachite, and azurite are specifically present in the leached zone. In the supergene and hypogene zones, sulfide minerals include pyrite, molybdenite, galena, sphalerite, marcasite, and copper sulfide minerals (i.e., chalcopyrite, bornite, chalcocite, and covellite) with different paragenesis. Kaolinite is present in both the supergene and hypogene zones, and native copper is also found between the leached and supergene zones. The main copper-bearing minerals of the Sungun porphyry deposit are sulfide minerals, most specifically chalcopyrite. Because flotation is the most common method for processing copper sulfide minerals, this method is used to process minerals from extracted ore in the Sungun porphyry copper processing complex [26].

2.2. Sample preparation

To investigate the effect of mineralogical and textural properties of sulfide minerals on the flotation process, a sample was collected from the flotation circuit of the Sungun copper concentration plant. Tables 1, 2, and 3 show the mineralogical and chemical composition of the feed sample, as determined by X-ray fluorescence (XRF) analysis.

Table 1. Mineralogical composition of the feed sample wt%

SiO_2	Al_2O_3	BaO	CaO	Fe_2O_3	K_2O	MgO	MnO	Na_2O	P_2O_5	SO_3	TiO_2	LOI
63.24	15.81	0.08	0.73	6.48	3.97	1.18	< 0.05	0.49	< 0.05	6.65	0.53	5.56

Note: LOI—Loss on ignition.

Table 2. Chemical composition of the feed sample 10^{-4}wt%

Ag	As	Cd	Ce	Co	Cr	Cu	La	Li	Mo	Ni	Pb	Sb
0.47	84.3	0.48	36	24	16	7761	22	2	117.4	44	65	21.9

Sc	Th	V	Y	Yb	Zn
1.2	11.1	12	5	0.6	91

Table 3. Microscopic studies of the feed sample

Minerals	Formula	Degree of liberation / %	d_{80} / μm
Chalcopyrite	$CuFeS_2$	95	150
Chalcocite	Cu_2S	85	100
Bornite	Cu_5FeS_4	83	110
Covellite	CuS	80	113
Pyrite	FeS_2	80	120

Note: d_{80} denotes 80% of the particles are smaller than this value.

To investigate the possibility of using the flotation method to recover particles smaller than 200 μm, the obtained sample, after being crushed by a jaw crusher, was ground in a mill to reduce its particle size to less than 200 μm. To determine the grain distribution range of the flotation circuit feed, wet screening analysis was performed using a set of sieves in accordance with the ASTM standard. The results of Smith's analysis are shown in Fig. 1. According to Fig. 1, the d_{80} of the particles is 112 μm (i.e., 80% of the particles are smaller than 112 μm).

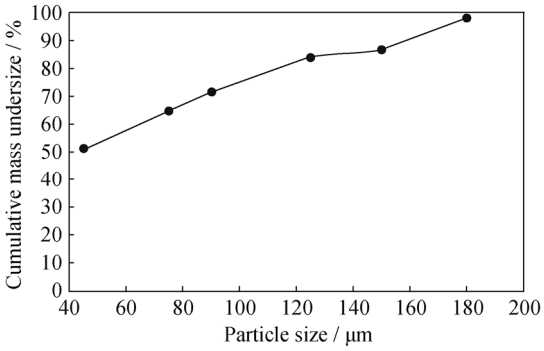

Fig. 1. Sieve analysis results of the flotation feed sample in the Sungun copper processing plant.

2.3. Flotation tests

Two flotation tests were conducted using the same flotation machine (Denver D12) with a 4.5-L cell and an agitation speed of 1200 r/min. In both replicates, the sample mass was 1175 g and the pH was adjusted to 10.5. In each test, after preparation of the pulp with a specific solids concentration (pulp density of 25wt% and 30wt%), Z11 (sodium isopropyl xanthate) and Flomin7240 (sodium di-*sec*-butyl dithiophosphate + sodium mercaptobenzothiazole) were added to the flotation cells as collectors. After 2 min, A70 (polypropylene glycol) and A65 (methyl isobutyl carbonyl) were added as frothers and mixed for approximately 1 min. In the next step, air was blown into the airflow and the process of dipping (or concentrating) was conducted at time periods of 20, 60, 180, 360, 600, and 900 s (Fig. 2).

All products of the tests were filtered, dried, and subsequently analyzed by atomic absorption spectrometry (AAS) to determine copper grade. The copper recovery (R) was calculated using Eq. (1):

$$R = \frac{Cc}{Ff} \times 100\% \quad (1)$$

where C is the dried concentrate mass, c is the concentrate grade, F is the feed mass, and f is the feed grade.

The results of the copper grade analysis and the calculated copper recovery at different sampling periods are presented at the Table 4. The separation efficiency was obtained for each individual process.

To determine mineralogical and textural characteristics of the concentrate and tails of each test, a thin section was prepared. The particle size, degree of liberation, and interaction of the valuable and gangue minerals were studied with a Leitz SM-LUX-POL microscope.

3. Results and discussion

3.1. Mineralogical and textural characteristics of concentrates and tails

Photomicrographs of the polished sections of the concentrates and tails of the flotation tests are shown in Figs. 3 and 4. The combinations of the concentrates were obtained at different time periods of 20, 60, 180, 360, 600, and 900 s. The mineralogical and textural characteristics of the concentrates in each time-period process and in the final tails are described and discussed in detail as follows:

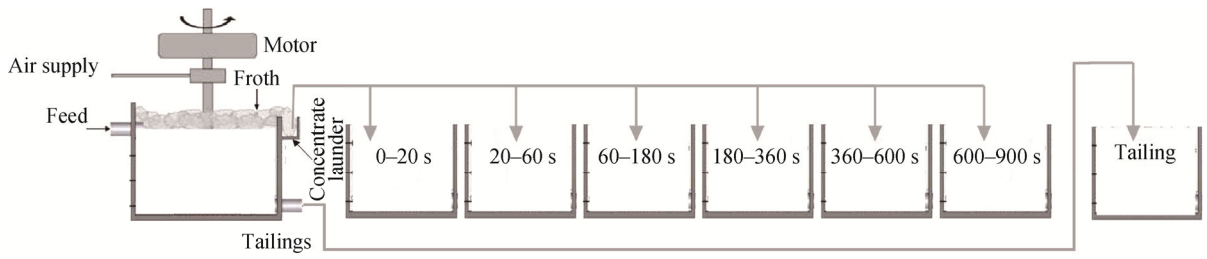

Fig. 2. Schematic of the flotation test method.

Table 4. Results of metallurgical accounting for flotation processes

Concentration sampling periods / s	Grade / %	Recovery / %	Pulp density / wt%	Total separation efficiency / %
0–20	11.39	22.96	25	26.84
20–60	10.87	14.61		
60–180	6.21	19.94		
180–360	3.56	11.16		
360–600	1.82	7.07		
600–900	1.21	4.70		
0–20	8.71	32.51	30	58.13
20–60	7.18	26.80		
60–180	3.84	21.79		
180–360	2.05	7.50		
360–600	1.21	7.05		
600–900	0.73	3.27		

As shown in Figs. 3(a) and 4(a), in the first concentrate of the flotation test, the pulp density was 25wt% and the copper sulfide minerals included chalcopyrite (56.2wt%), chalcocite (29.1wt%), covellite (6.4wt%), and bornite (4.7wt%). The order of these minerals' abundance in the test with a pulp density of 30wt% were approximately the same as in the first test. Chalcopyrite particles in this concentrate can be divided into two types based on their textural features: chalcopyrite without substitution and coated with other copper sulfide minerals (type A); and chalcopyrite that has interacted and is coated with other copper sulfides such as covellite (type B). Chalcopyrite particles in the concentrate of the flotation test with a pulp density of 25wt% exhibited a substantially different composition compared with the other copper sulfides. The chalcopyrite abundance (type A) in the test with a pulp density of 25wt% was substantially greater than that in the test with 30wt% (56.2wt% to 33.72wt%). With a decrease in the pulp density, the entrainment of fine particles into the concentrate was reduced and the efficiency of gangues drainage through the froth zone was improved. As a result, the grade of the target particles (chalcopyrite) increased in the concentrate. Pyrite was the main sulfide gangue mineral (3.6wt%) in concentrates in the first 20 s. The particle size of pyrite was in the range of 5 to 150 μm.

As shown in Figs. 3(b) and 4(b), the order of the copper sulfide minerals' abundance in this concentrate was similar to that in the concentrate obtained in the first 20 s of processing time. The concentrations of pyrite in this time period were substantially reduced (3.6wt% to 2.5wt%) compared with the concentrations in the first 20 s of processing. Because pyrite has a high floatability potential, in the primary stages of concentrating, the amount of floated pyrite was greater; as time went by, the amount of pyrite decreased. However, with increasing retention time, pyrite depression increased. As shown in Figs. 3(c) and 4(c), the order of the copper sulfide minerals' abundance in this concentrate was similar to those in the concentrates of 20 and 60 s. The amount of pyrite was lower in the concentrate at 180 s (2wt%) than in the concentrate at 60 s (2.5wt%).

As shown in Figs. 3(d) and 4(d), the order of the copper sulfide minerals' abundance in this concentrate was similar to that in the concentrates obtained at 180 s of processing time. Comparing the concentrations at 300 s of the flotation tests with pulp densities of 25wt% and 30wt% reveals that the amount of chalcopyrite and secondary copper sulfides such as chalcocite and covellite in the test with 25wt% pulp density was substantially lower compared with the amount in the test conducted with 30wt% pulp density. The amounts of chalcopyrite and secondary copper sulfide minerals in the tests with a pulp density of 25wt% and 30wt% were 34wt% and 50.1wt%, respectively. At 300 s in the test with a pulp density of 25wt%, the amount of chalcopyrite decreased; by contrast, in the test with a pulp density of 30wt%, because of the higher density of the pulp, the chalcopyrite concentration in the flotation cell was high.

As shown in Figs. 3(e) and 4(e), the copper sulfide minerals in this concentrate were similar to those in the concentrates obtained at other processing times. In this concentrate, because of the substantial loss of copper minerals (< 30wt%), the amount of pyrite was noticeably increased to 20wt%. As shown in Figs. 3(f) and 4(f), the order of the copper sulfide minerals' abundance and pyrite characteristics in this concentrate were similar to

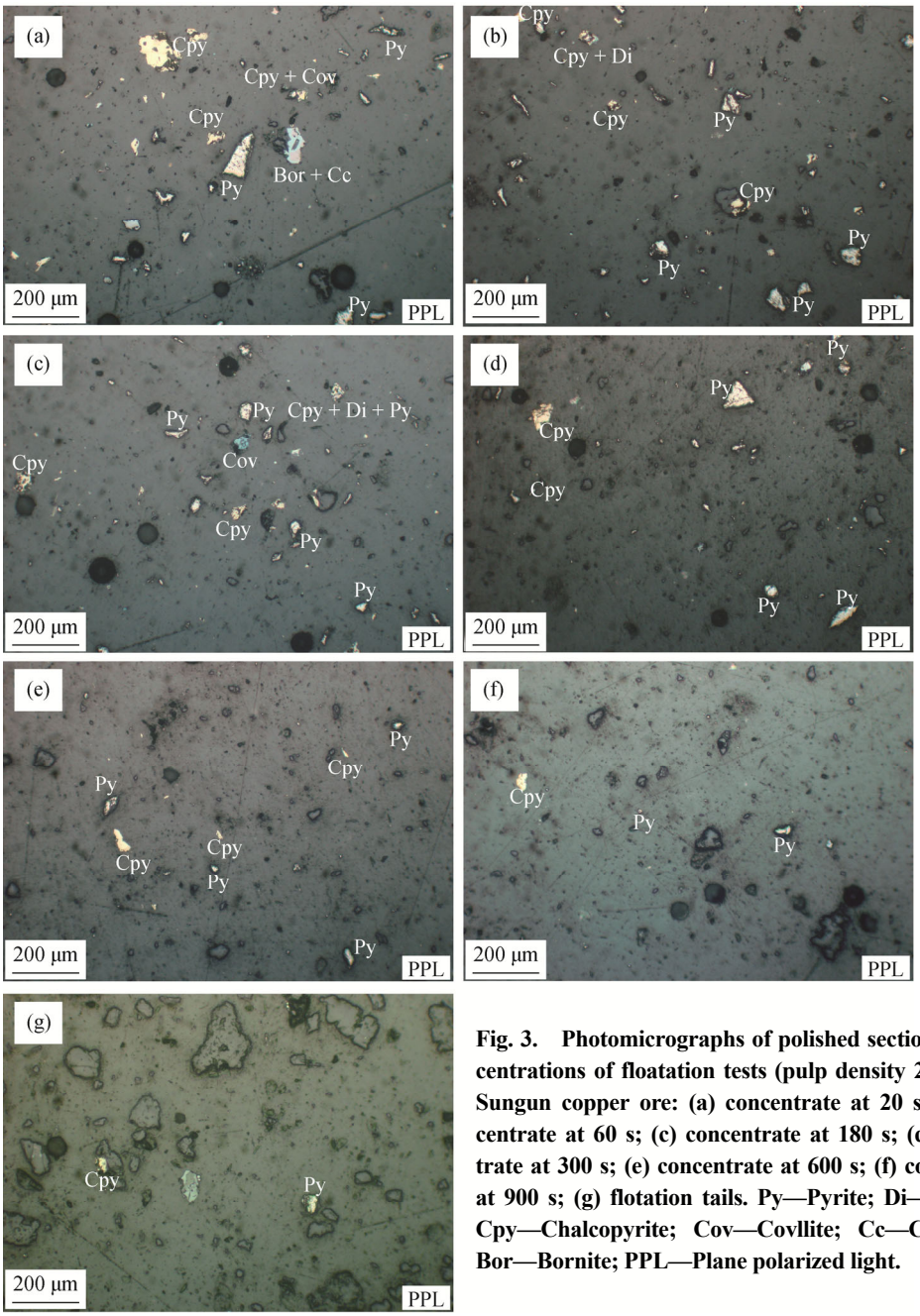

Fig. 3. Photomicrographs of polished sections of concentrations of floatation tests (pulp density 25wt%) in Sungun copper ore: (a) concentrate at 20 s; (b) concentrate at 60 s; (c) concentrate at 180 s; (d) concentrate at 300 s; (e) concentrate at 600 s; (f) concentrate at 900 s; (g) flotation tails. Py—Pyrite; Di—Digenite; Cpy—Chalcopyrite; Cov—Covllite; Cc—Chalcocite; Bor—Bornite; PPL—Plane polarized light.

that of the copper sulfide concentrates collected at different processing times. Flotation tails also included uncoated chalcopyrite particles and a smaller amount of secondary sulfides that were involved or coated with chalcopyrite. Chalcopyrite particles' size in the tailings was in the range from 10 to 25 μm. Because of the problems encountered in the processing of fine particles, particles smaller than 25 μm are usually introduced to tailings. Generally, in the flotation process, the largest recovery is achieved for particles between 250 and 106 μm [27]. This behavior indicates that the maximum combustible recovery was achieved in the rougher flotation stage with an intermediate particle size.

3.2. Degree of liberation in concentrates and tailings

The results of the concentrates' analysis and the textural features' studies of large particles show that high-grade concentrates can be produced if the valuable particles have a suitable degree of liberation (copper minerals). According to Pokrajcic [28], to produce a suitable product with high separation efficiency, the degree of liberation of the particles should be greater than 80%. On the basis of degree-of-liberation studies performed on the polished sections, chalcopyrite had a suitable degree of liberation (95%) in all of the concentrates.

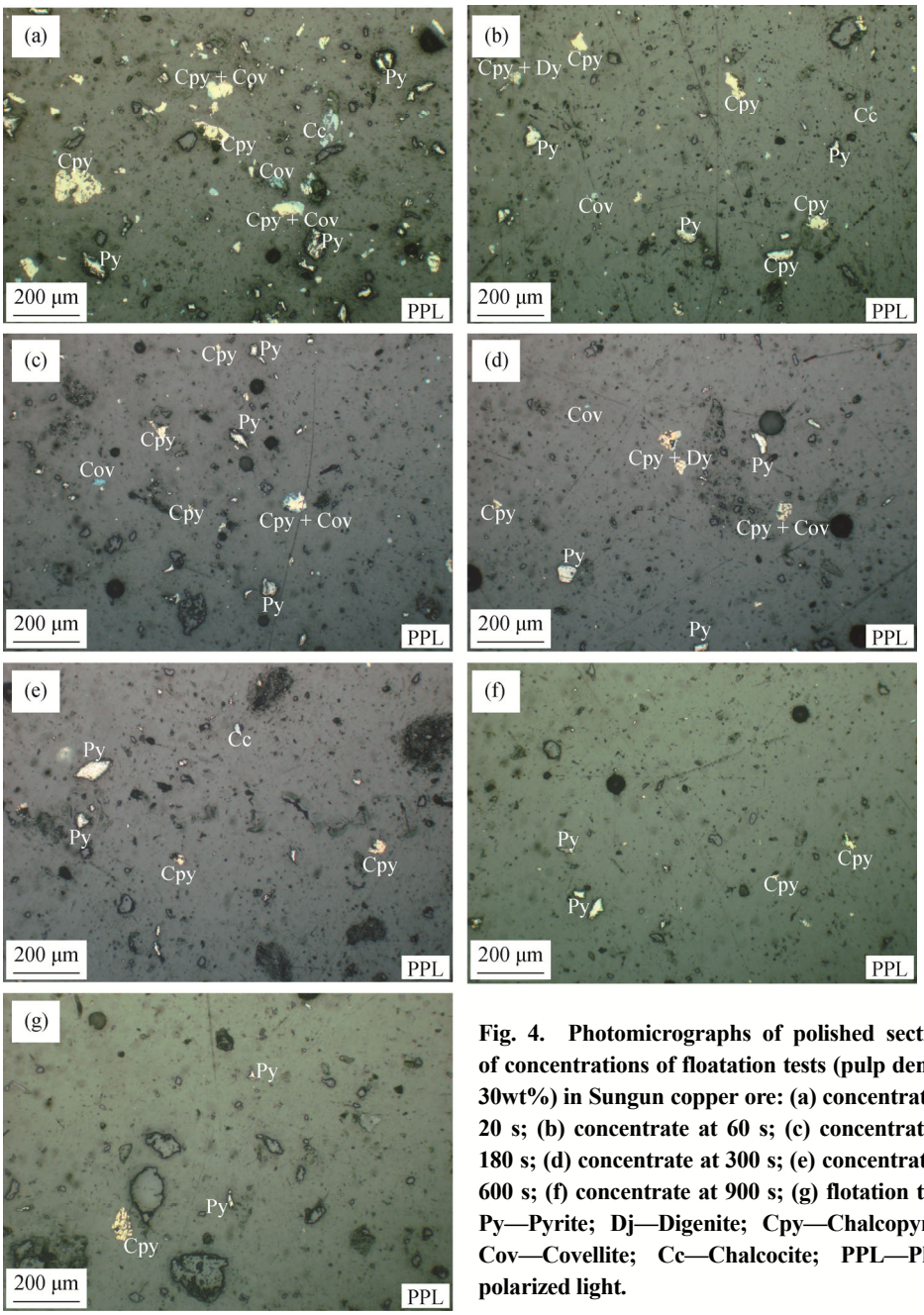

Fig. 4. Photomicrographs of polished sections of concentrations of floatation tests (pulp density 30wt%) in Sungun copper ore: (a) concentrate at 20 s; (b) concentrate at 60 s; (c) concentrate at 180 s; (d) concentrate at 300 s; (e) concentrate at 600 s; (f) concentrate at 900 s; (g) flotation tails. Py—Pyrite; Dj—Digenite; Cpy—Chalcopyrite; Cov—Covellite; Cc—Chalcocite; PPL—Plane polarized light.

Table 5 shows the ratio of pure chalcopyrite particles to locked chalcopyrite and other copper sulfide particles. During the concentration process of the test with a pulp density of 25wt%, the number of pure chalcopyrite particles decreases over time; in contrast, in the test with pulp density of 30wt%, the release of floating chalcopyrite increases over time. Therefore, at the early stages of the concentration process, the amount of floated chalcopyrite in the test with a pulp density of 25wt% was greater than the amount of floated chalcopyrite in the test with a pulp density of 30wt%. With further processing during the tests,

Table 5. Ratio of pure chalcopyrite particles to other copper sulfide and coated chalcopyrite particles

Time of concentration / s	Ratio / %	
	Test with pulp density of 25wt%	Test with pulp density of 30wt%
20	400–300	200
60	233.33	233.33–185.71
180	233.33	300
300	233.33–185.71	400–300
600	185.71–150	566.66
900	150	566.66–900

the amount of floated chalcopyrite in the test with a pulp density of 30wt% increases because of an increase in the degree of liberation of the chalcopyrite particles. In the tailings samples, pyrite particles showed a high degree of liberation (approximately 95%–90%).

3.3. Particle size of copper sulfide minerals at concentration time

Fig. 5 illustrates the variations in the d_{80} of the chalcopyrite particles. According to the Fig. 5, the d_{80} values of the concentrates obtained from the flotation test with a pulp density of 30wt% are greater than the d_{80} values of the concentrates obtained from the flotation test with a pulp density of 25wt%. In both flotation tests, as time passes, the d_{80} value decreases, expressing a downward trend in the particle size of chalcopyrite from the first concentrate to the final concentrate obtained at different processing time periods.

3.4. Recovery rates of concentrates based on the size of target minerals

The effect of the mineralogical properties of the ore sample, such as its particle size, on processing variables such as recovery and product has already been documented [29]. Fig. 6 shows the changes in the recovery and grade of copper sulfide minerals as functions of the d_{80} of the chalcopyrite particles. In both flotation tests, the grade and recovery increased with increasing particle size. With increasing chalcopyrite particle size, the particles become more likely to collide and attach to the air bubbles during the flotation process, thereby increasing both the grade and the recovery.

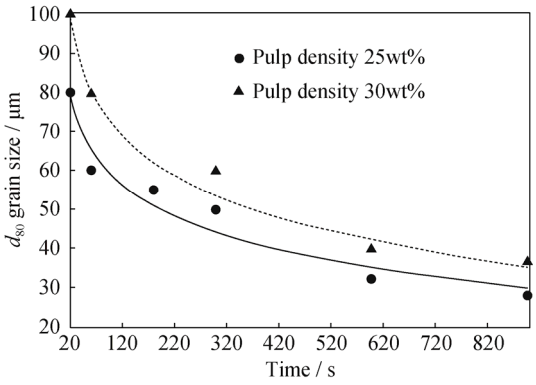

Fig. 5. d_{80} of chalcopyrite particles at different concentration times in flotation tests with different solids mass percentages.

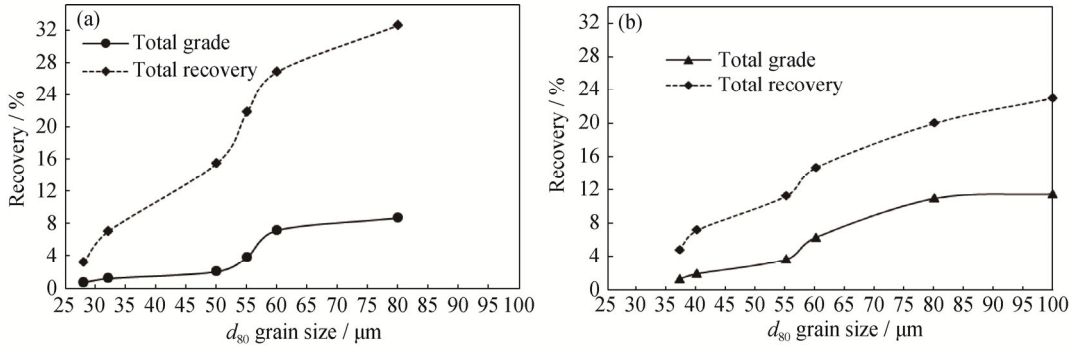

Fig. 6. Changes in recovery and grade versus the d_{80} of chalcopyrite particles (at 900 s): (a) flotation test with a pulp density of 25wt%; (b) flotation test with a pulp density of 30wt%.

Fig. 7 illustrates how a particle affects the recovery curve. On the basis of the theoretical curve of Fig. 7, if the compound composition of the complex mineralogy and the flow of the feed are constant, then the grade will decrease. Similarly, if the flow of the feed contains free particles, the curve will be angled. In Fig. 7(b), point 1 indicates the position of the real recovery curve and the operating conditions that will change with changes in the position of the operation process. Point 2 is related to the potential for the degree of liberation, which will change in response to a change in the milling conditions and classification (this curve does not include naturally floated unwanted gangue particles) [30].

Fig. 8 shows a graph of the grade as a function of the recovery for the Sungun copper flotation tests. According to Fig. 8, with increasing concentrating time, the copper grade decreases and the recovery increases. The recovery rate and grade could be increased by changing the operating conditions of the flotation test in the test with a pulp density of 30wt%. With regard to the flotation test with a pulp density of 25wt%, the change in recovery rates and grade depends on an increase in the degree of liberation of the feed by changing the milling conditions and classification.

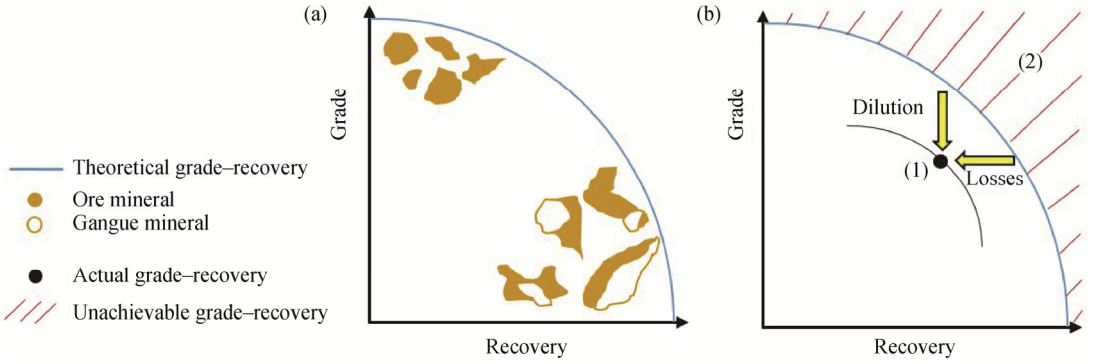

Fig. 7. Schematic of the (a) theoretical grade–recovery curve and (b) actual and unachievable grade–recovery adopted from [31].

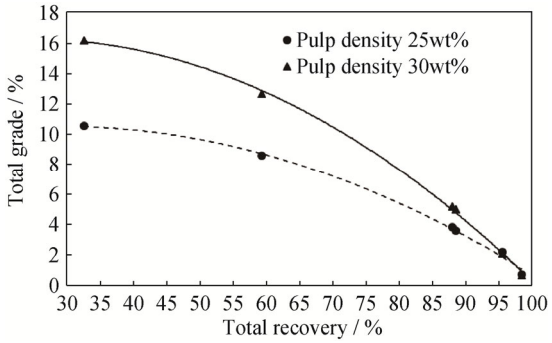

Fig. 8. Grade–recovery graph corresponding to the flotation tests.

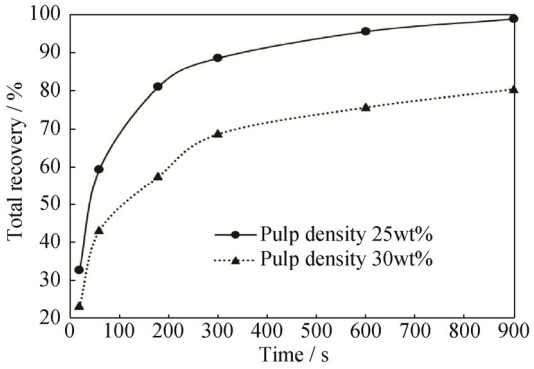

Fig. 9. Results of the recovery rates of the concentrates at different time intervals.

3.5. Kinetics of flotation–granulation distribution

The flotation kinetics of sulfide minerals are well known to be affected by their particle size [32–33]. A kinetics study of the flotation process includes determining all of the factors that influence the amount of concentrate. Concentrate production can be defined in various ways, but it is generally presented as recovery as a function of time. In Fig. 9, the graph of the recovery at different concentration times is shown for each flotation test performed. Various kinetics models have been suggested for analyzing batch flotation test results [23,25]. To calculate the kinetic parameters for the Sungun copper flotation feed, the results of the flotation test data were fitted to the classic, Klimpel, fully mixed reactor model, the improved gas/solid adsorption model, and the rectangular distribution model and the associated parameters were calculated [22,24–25]. According to nonlinear multivariable regression, the results match very well with the rectangular-distribution second-order kinetic model as shown in Eq. (2):

$$R = R_{\infty}\left(1-\frac{1}{kt}(\ln(1+kt))\right) \qquad (2)$$

where R denotes recovery, R_{∞} denotes infinite recovery, k is rate of flotation and t is time.

Fig. 10 shows the flotation-rate graphs in terms of the d_{80} of the chalcopyrite particles. In each test, with an increase in d_{80} of the chalcopyrite particles, the flotation rate constant increases and, after reaching a maximum value, trends downward. In both flotation tests, the maximum constant of flotation occurs at d_{80} between sizes 55 and 50 μm. Thus, the optimal size distribution range to achieve the maximum flotation rate is 50–55 μm, in agreement with previous studies in which the maximum flotation recovery and flotation constant in tests were observed for particles smaller than 106 μm [34].

4. Conclusions

In this study, process mineralogy is applied as a predictive and practical tool for further understanding and predicting the flotation kinetics of the copper sulfide minerals. Sample characterizations such as the mineral composition and association and the grain distribution and liberation within the ore samples were conducted for the feed, the concentrates obtained at different processing times, and the tailings of the flotation processes (with different pulp densities of 25wt% and 30wt%) of copper sulfide. The obtained results are summarized as follows:

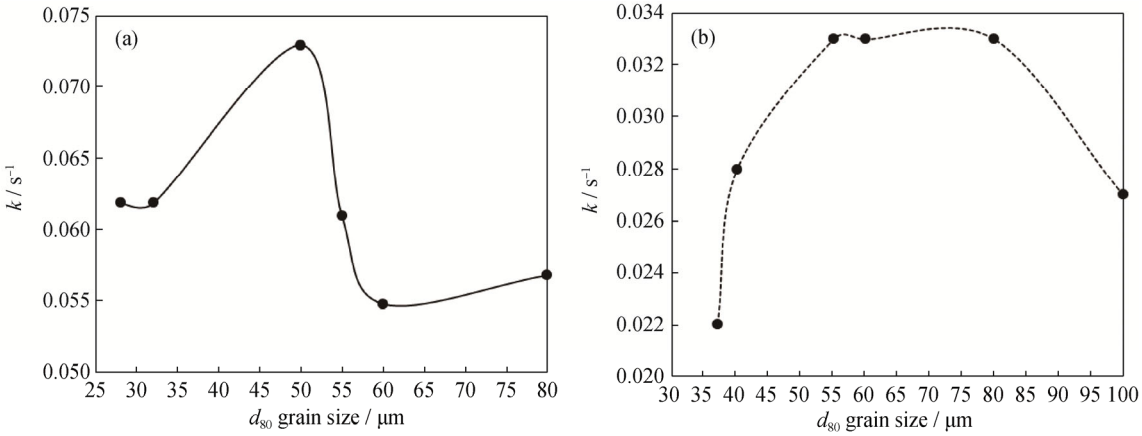

Fig. 10. Diagrams of the flotation rate constant as a function of chalcopyrite d_{80} grain size: (a) flotation test with a pulp density of 25wt%; (b) flotation test with a pulp density of 30wt%.

(1) The floated sulfide minerals were chalcopyrite (56.2wt%), chalcocite (29.1wt%), covellite (6.4wt%), and bornite (4.7wt%). The amounts of theses minerals in the concentrates began decreasing as the flotation process continued. Pyrite was the main sulfide gangue mineral (3.6wt%) in the concentrates.

(2) According to the analysis results, the major copper-bearing mineral in the Sungun ore deposit is chalcopyrite. Chalcopyrite had the highest recovery (56.2%) in the flotation test performed on the sample with a d_{80} between 80 and 100 μm. The degree of liberation of chalcopyrite, in this case, was approximately 95%. Chalcopyrite particles with a d_{80} greater than 100 μm were recovered at the early stages of the flotation process.

(3) According to the kinetic studies, the second-order rectangular distribution model perfectly matched the flotation test data. Further examination of the kinetic parameters indicated that the optimum size distribution range to achieve a maximum flotation rate for chalcopyrite particles was between 50 and 55 μm.

(4) According to the obtained results, the best method to predict the flotation kinetics of copper sulfide minerals is to conduct a comprehensive study of their grain distribution, grain liberation, and associated minerals, in conjunction with optimal grinding and regrinding circuit design. This approach will help achieve constructive flotation kinetics in the processing of copper sulfide minerals.

(5) As the main outcome of this research, we strongly recommend designing an appropriate ore processing system. In addition, the concentration of minerals within a deposit requires full comprehensive process mineralogy study to achieve desirable and more efficient operating conditions.

References

[1] N.O. Lotter, Modern process mineralogy: An integrated multi-disciplined approach to flow sheeting, *Miner. Eng.*, 24(2011), No. 12, p. 1229.

[2] N.O. Lotter, L.J. Kormos, J. Oliveira, D. Fragomeni, and E. Whiteman, Modern process mineralogy: Two case studies, *Miner. Eng.*, 24(2011), No. 7, p. 638.

[3] C.P. Brough, R. Warrender, R.J. Bowell, A. Barnes, and A. Parbhakar-Fox, The process mineralogy of mine wastes, *Miner. Eng.*, 52(2013), p. 125.

[4] C. Rule and R.P. Schouwstra, Process mineralogy delivering significant value at anglo platinum concentrators operations, [in] *The 10th International Congress for Applied Mineralogy (ICAM)*, Trondheim, 2011, p. 613.

[5] N.O. Lotter, W. Baum, S. Reeves, C. Arrué, and D.J. Bradshaw, The business value of best practice process mineralogy, *Miner. Eng.*, 116(2018), p. 226.

[6] J. Zhou and Y. Gu, Gold process mineralogy and its significance in gold metallurgy, [in] *The 9th International Congress for Applied Mineralogy (ICAM)*, Brisbane, 2008, p. 205.

[7] L.J. Cabri, M. Beattie, N.S. Rudashevsky, and V.N. Rudashevsky, Process mineralogy of Au, Pd and Pt ores from the Skaergaard intrusion, Greenland, using new technology, *Miner. Eng.*, 18(2005), No. 8, p. 887.

[8] R.J. Bowell, J. Grogan, M. Hutton-Ashkenny, C. Brough, K. Penman, and D.J. Sapsford, Geometallurgy of uranium deposits, *Miner. Eng.*, 24(2011), No. 12, p. 1305.

[9] P.R. Alves, *The Carbonatite-Hosted Apatite Deposit of Jacu-*

piranga, SE Brazil: Styles of Mineralization, Ore Characterization, and Association with Mineral Processing [Dissertation], Missouri University of Science and Technology, Rolla, 2008.

[10] M. Becker, C. Brough, D. Reid, D. Smith, and D. Bradshaw, Geometallurgical characterisation of the Merensky Reef at Northam platinum mine–comparison of Normal, Pothole and Transitional reef types, [in] *The 9th International Congress for Applied Mineralogy (ICAM)*, Brisbane, 2008, p. 391.

[11] D. Uliana, M.M.M.I. Tassinari, H. Kahn, and B.K. Hashizume, Process mineralogy studies of low grade iron ores used in the production of pellet feed, [in] *The 10th International Congress for Applied Mineralogy (ICAM)*, Trondheim, 2011, p. 717.

[12] D. Chetty, W. Clark, and M. Kotze, Process mineralogical studies in the beneficiation of rare earth element ores, [in] *Process Mineralogy '12*, Cape Town, 2012, p. 136.

[13] E. Donskoi, R.J. Holmes, J.R. Manuel, J.J. Campbell, A. Poliakov, S.P. Suthers, and T.D. Raynlyn, Utilisation of iron ore texture information for prediction of downstream process performance, [in] *The 9th International Congress for Applied Mineralogy (ICAM)*, Brisbane, 2008, p. 687.

[14] C.R. McClung and F. Viljoen, Mineralogical assessment of the metamorphosed broken hill sulphide deposit, South Africa: Implications for processing complex ore bodies, [in] *The 10th International Congress for Applied Mineralogy (ICAM)*, Trondheim, 2011, p. 427.

[15] D. Meadows, D. Jensen P. Thompson, W. Baum, S. Yu, Mineralogical influences on copper, molybdenum and gold flowsheets: an overview, [in] *Process Mineralogy '12*, Cape Town, 2012, p. 146.

[16] A. Rozendaal and R.G. Horn, Mineralogy and recovery of copper from smelter slag of the O'Okiep Copper District, South Africa, [in] *Process Mineralogy '12*, Cape Town, 2012, p. 10.

[17] W. Thompson, A. Lombard, E. Santiago, and A. Singh, Mineralogical studies in assisting beneficiation of rare earth element minerals from carbonatite deposits, [in] *The 10th International Congress for Applied Mineralogy (ICAM)*, Trondheim, 2011, p. 665.

[18] Y. Ghorbani, M. Becker, J. Petersen, A.N. Mainza, and J.P Franzidis, Investigation of the effect of mineralogy as rate-limiting factors in large particle leaching, *Miner. Eng.*, 52(2013), p. 38.

[19] Y. Ghorbani, R. Fitzpatrick, M. Kinchington, G. Rollinson, and P. Hegarty, A process mineralogy approach to gravity concentration of Tantalum bearing minerals, *Minerals*, 7(2017), No. 10, p. 194.

[20] L. Reyes-Bozo, R. Herrera-Urbina, C. Sáez-Navarrete, A.F. Otero, A. Godoy-Faúndez, and R. Ginocchio, Rougher flotation of copper sulphide ore using biosolids and humic acids, *Miner. Eng.*, 24(2011), No. 14, p. 1603.

[21] H.J. Zhang, J.T. Liu, Y.J. Cao, and Y.T. Wang, Effects of particle size on lignite reverse flotation kinetics in the presence of sodium chloride, *Powder Technol.*, 246(2013), p. 658.

[22] A. Azizi, A. Hassanzadeh, and B. Fadaei, Investigating the first-order flotation kinetics models for Sarcheshmeh copper sulfide ore, *Int. J. Min. Sci. Technol.*, 25(2015), No. 5, p. 849.

[23] H. Vapur, O. Bayat, and M. Uçurum, Coal flotation optimization using modified flotation parameters and combustible recovery in a Jameson cell, *Energy Convers. Manage.*, 51(2010), No. 10, p. 1891.

[24] M. Gharai and R. Venugopal, Modeling of flotation process—an overview of different approaches, *Miner. Process. Extr. Metall. Rev.*, 37(2016), No. 2, p. 120.

[25] J. Drzymala, T. Ratajczak, and P.B. Kowalczuk, Kinetic separation curves based on process rate considerations, *Physicochem. Probl. Miner. Process.*, 53(2017), No. 2, p. 983.

[26] K. Ismaili, and F. Mar, Investigation on the enrichment of heavy metals caused by Sungun copper deposit in drainage sediments, *Iran. J. Min. Eng.*, 17(2012), No. 7, p. 33.

[27] C. Ni, G.Y. Xie, M.G. Jin, Y.L. Peng, and W.C. Xia, The difference in flotation kinetics of various size fractions of bituminous coal between rougher and cleaner flotation processes, *Powder Technol.*, 292(2016), p. 210.

[28] Z. Pokrajcic, *A Methodology for the Design of Energy Efficient Commination Circuits* [Dissertation], The University of Queensland, Brisbane, 2010.

[29] L. Lorenzen and M.J. Barnard, Why is mineralogical data essential for designing a metallurgical test work program for process selection and design? [in] *The First AusIMM International Geometallurgy Conference*, Brisbane, 2011.

[30] D. Bradshaw, The role of process mineralogy in improving the process performance of complex sulphide ores, [in] *Proceedings of the XXVII International Mineral Processing Congress*, Santiago, 2014.

[31] A.F. Cropp, W.R. Goodall, and D.J. Bradshaw, The influence of textural variation and gangue mineralogy on recovery of copper by flotation from porphyry ore—a review, [in] *The Second AusIMM International Geometallurgy Conference*, Brisbane, 2013, p. 279.

[32] E. Whiteman, N.O. Lotter, and S.R. Amos, Process mineralogy as a predictive tool for flowsheet design to advance the Kamoa project, *Miner. Eng.*, 96-97(2016), p. 185.

[33] N.W. Johnson, Existing methods for process analysis, [in] C.J. Greet, Ed., *Flotation Plant Optimization: a Metallurgical Guide to Identifying and Solving Problems in Flotation Plants*, The Australasian Institute of Mining and Metallurgy, Perth, 2010, p. 35.

[34] F. Kazemi, A. Bahrami, and J. Abdolahi Sharif, Determination of the difference in recovery and kinetics of various size fractions of gilsonite in rougher and cleaner flotation processes, *Int. J. Min. Geo-Eng.*, 53(2019). https://doi.org/10.22059/IJMGE.2018.256299.594732.